Direct Observation of Hydrogen-Bond Exchange within a Single Water Dimer

T. Kumagai, M. Kaizu, S. Hatta, H. Okuyama,* and T. Aruga
Department of Chemistry, Graduate School of Science, Kyoto University, Kyoto 606-8502, Japan

I. Hamada and Y. Morikawa
The Institute of Scientific and Industrial Research, Osaka University, 8-1 Mihogaoka, Ibaraki Osaka 567-0047, Japan

(Received 24 January 2008; published 24 April 2008)

The dynamics of water dimers was investigated at the single-molecule level by using a scanning tunneling microscope. The two molecules in a water dimer, bound on a Cu(110) surface at 6 K, were observed to exchange their roles as hydrogen-bond donor and acceptor via hydrogen-bond rearrangement. The interchange rate is ~60 times higher for $(H_2O)_2$ than for $(D_2O)_2$, suggesting that quantum tunneling is involved in the process. The interchange rate is enhanced upon excitation of the intermolecular mode that correlates with the reaction coordinate.

DOI: 10.1103/PhysRevLett.100.166101 PACS numbers: 68.43.−h, 68.37.Ef, 68.47.De

The structure and dynamics of water dimers have been subjects of extensive research as a prototype of much more complex hydrogen-bonding systems [1,2]. The water molecules in a free water dimer rearrange the hydrogen bond through quantum tunneling among eight equivalent structures, which causes the tunneling splittings in the vibration-rotation spectra [2]. One of the rearrangement pathways is the interchange of the hydrogen-bond donor and acceptor molecules, in which the roles of the donor and acceptor molecules are exchanged via concerted rotation. The tunneling rate for this motion was determined from the tunneling splitting to be $10^9\ \mathrm{s}^{-1}$ for $(H_2O)_2$ [2]. The effect of vibrational excitation on the interchange tunneling dynamics was also investigated [3]. The tunneling splitting was found to change drastically upon the excitation of the intermolecular vibrational mode that was argued to correlate with the interchange reaction coordinate.

The interchange motion was recently invoked to explain the unique mobility of water dimers on the Pd(111) surface [4,5]. Water dimers are bonded with the surface mainly via the oxygen atom of the donor molecule, and the free azimuthal rotation of the acceptor molecule around the donor molecule combined with facile interchange results in the unexpectedly rapid diffusion of water dimers over Pd(111) [4].

The dynamics of the hydrogen-bond exchange at solid surfaces has not yet been understood, although it plays important roles in, e.g., catalytic reaction. In this study, the interchange motion was directly observed for individual water dimers on Cu(110) by using a scanning tunneling microscope (STM). The substrate has an up-and-down, washboard structure of large corrugation, where the rotation and diffusion of water dimers are inhibited, thereby making the interchange process accessible. The interchange motion was monitored in real time. A large isotope effect was found in the interchange rate, which corroborates the hydrogen-atom tunneling involved in the process. Furthermore, the interchange motion was found to be coupled with the intermolecular vibration, based on which we propose a mechanism of vibrationally assisted tunneling.

The experiments were carried out in an ultrahigh-vacuum chamber equipped with an STM (Unisoku, USM-1200). The STM images were acquired in constant current mode at 6 K. An electrochemically etched tungsten tip was used as an STM probe. A single-crystalline Cu(110) was cleaned by repeated cycles of argon ion sputtering and annealing. The surface was exposed to H_2O or D_2O gases via a tube doser positioned ~1 cm apart from the sample surface at 12 K. We conducted the experiments at very low coverages, where water molecules exist mainly as isolated monomers or dimers. The calculations were based on the density functional theory using a plane-wave, pseudopotential code STATE [6]. We used five-layer Cu slabs with surface water dimers arrayed in a 2×3 surface unit cell and a k-space sampling at 16 points. Adsorbates and two top Cu layers were relaxed. The STM simulation based on the Tersoff-Hamann approach [7] was conducted with a 3×4 unit cell and finer 64 k points. In the calculation of the images shown below, the sample bias voltage and the tip height were set at 24 mV and 0.5 nm, respectively. We confirmed that the qualitative features were not affected by the tip height. The vibrational mode analysis was carried out by diagonalizing the dynamical matrices obtained by displacing each atom in the top Cu layer and adsorbates by 0.02 nm. The molecular graphics were produced by the XCRYSDEN graphical package [8].

Figure 1(a) shows a typical image of water monomers (H_2O) located on top of Cu atoms. The molecules were then forced to migrate along the atomic row (the $[1\bar{1}0]$ direction) by scanning the surface at a high (54 mV) sample bias, and two monomers encountered each other to yield a dimer [Fig. 1(b)]. The spontaneous dimerization is restricted due to the low mobility of the monomers at 6 K. The dimer is characterized by its intermittently fluc-

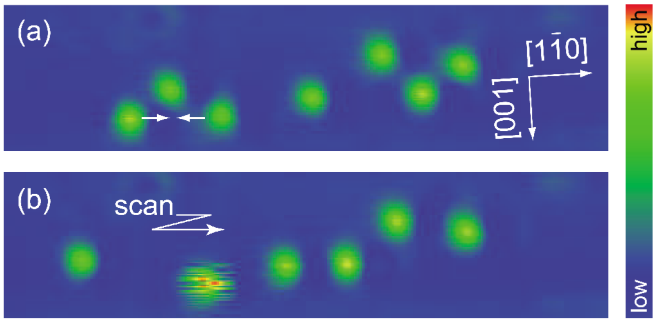

FIG. 1 (color online). (a) Constant current image of H_2O monomers. The image was acquired at 0.5 nA tunneling current and 24 mV sample bias. (b) An image after the area was scanned at 0.5 nA and 54 mV. This image was acquired at 0.5 nA and 24 mV. The 54 mV scan induced the monomers to migrate and form a dimer (fluctuating image). The apparent heights of the monomer and dimer are 60 and 80 pm, respectively. Each image size is $4 \times 16\ \mathrm{nm}^2$.

tuating image. Since the surface was scanned horizontally from the top to bottom, the fluctuating image indicates the bistable motion of the dimer along the $[1\bar{1}0]$ direction. Once the dimer is formed, it was never dissociated spontaneously, suggesting that the dimer is energetically preferred to the isolated monomers. The dissociation can be induced by applying a voltage pulse of ~0.2 V onto the dimer.

The STM image of the dimer shows dramatic change upon substitution with heavy water. Figure 2(a) shows STM images simultaneously acquired for $(H_2O)_2$ and $(D_2O)_2$. The D_2O dimer appears stationary, in contrast to the H_2O dimer, with an asymmetric "egg" shape with the long axis along the $[1\bar{1}0]$ direction. The asymmetry is also discernible for each envelope of the fluctuating bistable states of the H_2O dimer, indicating the same origin but different dynamical properties of these two species. An enlarged image for $(D_2O)_2$ is shown in Fig. 2(b). The grid lines represent the lattice of Cu(110). The long axis of the egg-shaped dimer is aligned on the atomic row. The dimer flips between two equivalent orientations, and the counterpart is shown in Fig. 2(d). Figure 2(c) shows the dimer which underwent flip-flop motion between the two orientations as the tip was scanned across it.

The stable structure of water dimer on Cu(110) was calculated by density functional theory, which is shown in Figs. 3(a) (side view) and 3(b) (top view). The lower-lying molecule (hydrogen-bond donor) is directly bonded to the Cu atom, while the higher-lying molecule (hydrogen-bond acceptor) interacts weakly with the substrate. The vertical displacement between the molecules is 0.067 nm, and the adsorption energy is 56 kJ/mol with respect to the free dimer [9]. Similar structures have been proposed for water dimers on close-packed metallic surfaces [4,10,11]. Figure 3(c) shows the STM image calculated for this structure. The image is characterized by the large and small protrusions over the acceptor and donor molecules, respectively. The former reflects mainly the $1b_1$ orbital (lone pairs) of the acceptor hybridized with substrate states. The simulation well reproduces the experimental image, and it is now clear that the bistable fluctuation of the water dimer is ascribed to the concerted motion of the two molecules that interchange their roles as donor and acceptor. We note that the interchange proceeds through the hydrogen-bond rearrangement; the isotope effect observed in the motion rules out the mutual interchange of the two water molecules.

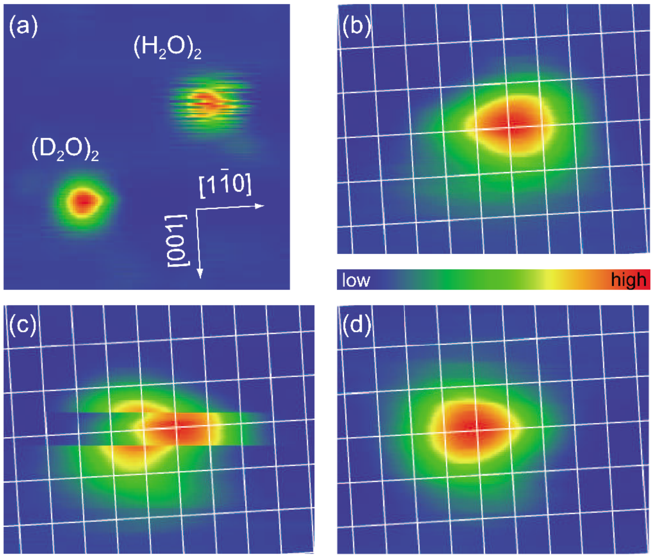

FIG. 2 (color online). (a) Constant current image simultaneously acquired for H_2O and D_2O dimers ($5.5 \times 5.5\ \mathrm{nm}^2$). (b) An enlarged image of the D_2O dimer ($2.4 \times 2.0\ \mathrm{nm}^2$). The asymmetric egg shape reflects the donor-acceptor configuration of the water dimer along $[1\bar{1}0]$. The grid lines represent the lattice of Cu(110) that is depicted through nearby monomers centered on top of Cu atoms. (c) The D_2O dimer flipped between the two orientations as the tip was scanned horizontally across it. (d) The counterpart of (b) in the same area. All images were acquired at 24 mV sample bias. Tunneling current was 0.5 nA for (a) and 0.3 nA for (b)–(d).

The temporal evolution of the interchange motion was studied by monitoring the tunneling current over the dimer with the feedback turned off. The typical result is shown in Fig. 4(a) for $(H_2O)_2$. The sample bias during the measurement was 24 mV. The jumps in the current correspond to the individual interchange events within the dimer. The distribution of the time intervals between the events obtained at three different tunneling currents is shown in Fig. 4(b). The data show linear slopes, which were used to determine the interchange rate. The rate was independent of the tunneling current, indicating that the tip effect on the interchange motion is negligible under the tunneling condition employed. Accordingly, the interchange rate was determined to be $(6.0 \pm 0.6) \times 10^1\ \mathrm{s}^{-1}$ for $(H_2O)_2$. The rate for $(D_2O)_2$ was determined to be $1.0 \pm 0.1\ \mathrm{s}^{-1}$ in a

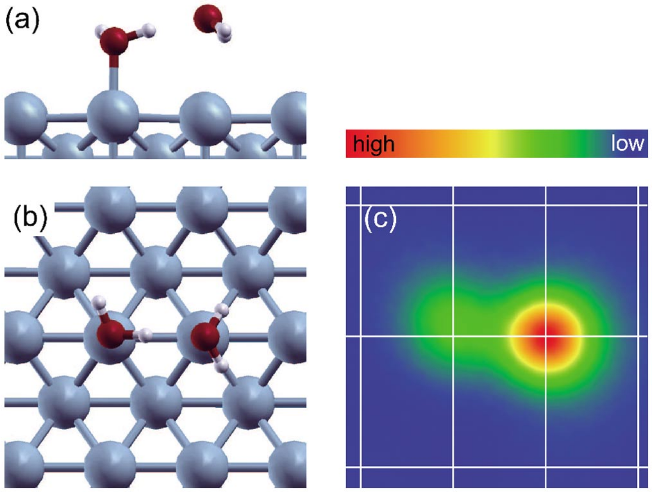

FIG. 3 (color online). (a) The calculated structure of water dimer on Cu(110) (side view). (b) The same as in (a) from top view. The Cu-O distances for the donor and acceptor molecules are 0.212 and 0.289 nm, respectively. The intermolecular O-O distance is 0.272 nm. (c) The calculated STM image corresponding to (b). The grid lines represent the lattice of Cu(110).

similar way. The large isotope effect (~ 60) suggests that the rate-limiting process involves quantum tunneling. The interchange proceeds via the transition state of C_2 symmetry [Fig. 4(f)], and the barrier is calculated to be 23 kJ/mol on Cu(110) while it is 21 kJ/mol on Pd(111) [4]. These cannot be overcome via mere thermal process, which corroborates that the interchange proceeds via tunneling. The interchange tunneling was manifest for gas-phase water dimers as tunneling splittings corresponding to $\sim 10^9$ s^{-1} for $(H_2O)_2$. The reduction of the rate by 7 orders of magnitude partly arises from the increase in the barrier height from 2.48 kJ/mol (gas-phase value [2]) to 23 kJ/mol. In contrast to the case of free dimers, the interchange reaction requires substantial displacement of oxygen atoms for the dimers adsorbed on the surface. The oxygen atoms have to be displaced in such a way that they are at the same height—only then might the interchange tunneling occur. For water dimers on Pd(111), the interchange process was argued to be separatable into two pathways with classical and quantum motions: The acceptor molecule is first brought to the same height with the donor molecule, and then the concerted rotation through tunneling results in the interchange [4]. This model succeeded in rationalizing a higher mobility of water dimer than the monomer on Pd(111) at 40 K [5]. In the present case (6 K), however, the displacement of the acceptor molecule may be restricted because it requires 8 kJ/mol. We propose that the tunneling proceeds along the optimal directions on the multidimensional potential energy surface with motions not only of hydrogen but also of oxygen atoms [12]. Thus the reduction of the interchange rate from the free dimer is ascribed to this mass effect. The multi-

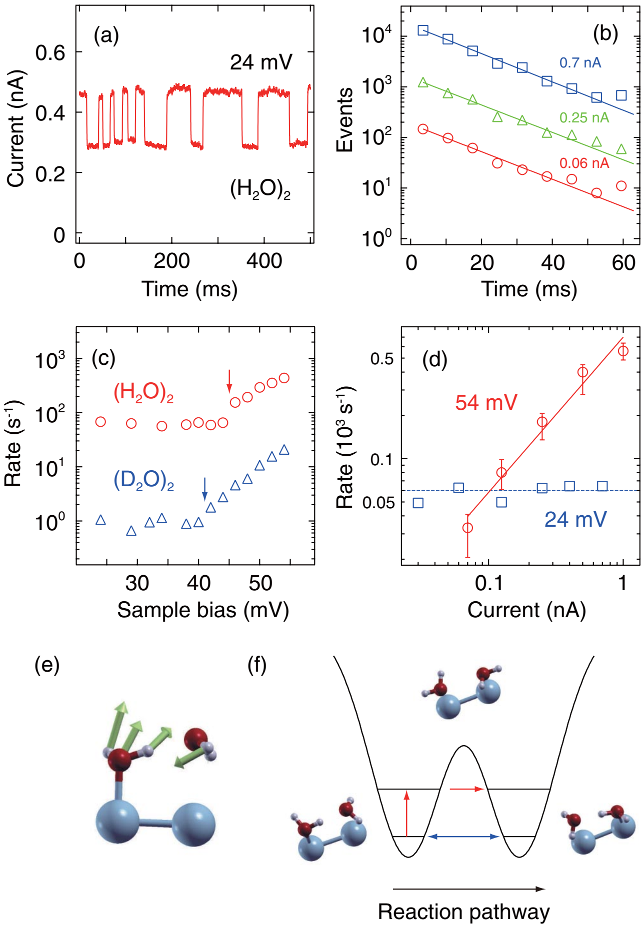

FIG. 4 (color online). (a) Typical tunneling current recorded with the tip fixed over the H_2O dimer. The tip was slightly displaced from the center of the dimer along $[1\bar{1}0]$. The sample bias during the measurement was 24 mV. The current jumps between the two states at the moments of interchange. (b) Distribution of the times for the dimer to stay at the two states. The tip height was varied so that the tunneling current was 0.06, 0.25, and 0.7 nA for the high-current state. The latter two data are displaced vertically for clarity. (c) Voltage dependence of the interchange rate for H_2O dimer (open circles) and D_2O dimer (open triangles). The tip height was adjusted to give 0.5 ± 0.1 nA for the high-current state whose distribution was used to obtain the rate. The arrows indicate the threshold voltages at which the rate starts to increase. The thresholds were determined to be 45 ± 1 and 41 ± 1 mV for $(H_2O)_2$ and $(D_2O)_2$, respectively. (d) Current dependence of the interchange rate at 24 mV (open squares) and 54 mV (open circles) for $(H_2O)_2$ in a logarithmic scale. The slope for the latter is unity. (e) A normal mode for $(H_2O)_2$ that couples with the interchange reaction. This mode involves the motions of donor-substrate stretch and acceptor rotation. (f) A schematic diagram of the potential energy along the interchange reaction pathway. The transition state is of C_2 symmetry with the Cu-O distances of 0.226 nm. In addition to the intrinsic tunneling between the ground states (blue or dark gray double-ended arrow), the interchange is mediated by the vibrational excitation (red or light gray arrows). The potential barrier is 23 kJ/mol (0.24 eV) while the vertical scale is not realistic.

dimensional treatment of the tunneling process is essential for the quantitative description of the interchange motion.

The interchange rate was obtained as a function of the applied bias voltage [Fig. 4(c)]. While the interchange motion is intrinsic at low bias voltage, as indicated by negligible tip effect, it becomes tip assisted at voltages higher than 40 mV. The threshold voltage is determined to be 45 ± 1(41 ± 1) mV for H_2O (D_2O) dimers. The dependence of the rate of the tip-induced motion on the tunneling current is shown in Fig. 4(d). The interchange rate was obtained at 54 mV sample bias as a function of tunneling current, from which the intrinsic contribution (60 s^{-1}) was subtracted to evaluate the rate of the induced motion. The linear dependence indicates that the interchange is induced via a single-electron process. For reference, the rate obtained at 24 mV sample bias is also shown in the figure, indicating no dependence on the tunneling current. We propose that molecular vibration is excited via inelastic electron tunneling that eventually leads to the interchange motion. The isotopic ratio of the threshold voltages (~ 1.1) suggests that the vibrational mode involves hindered translation of water molecules predominantly. We assign the mode to motions of donor-substrate stretch and acceptor rotation [Fig. 4(e)]. The corresponding vibrational energies were determined to be 36 and 34 meV for $(H_2O)_2$ and $(D_2O)_2$, respectively, by the normal-mode analysis. The other intermolecular modes are much lower in energy. This mode directly correlates with the interchange reaction coordinate. Since the barrier for the interchange (0.24 eV) is much larger than the energy transferred from a tunneling electron (45 meV), the electron-induced interchange has to proceed through tunneling. Figure 4(f) shows a schematic diagram of the potential energy along the interchange pathway. We propose that the interchange tunneling is assisted by the vibrational excitation (red or light gray arrows). The reaction yield [related to the increase in the rate in Fig. 4(c)] is ~20 times higher for $(H_2O)_2$ than $(D_2O)_2$, which is consistent with this mechanism. For the gas-phase water dimer, the tunneling splitting changes drastically upon excitation of molecular vibration [3]. Based on the argument that the vibration should correlate with the interchange reaction coordinate, it was assigned to the wagging mode of the acceptor molecule. Since the interchange for the adsorbed dimer requires not only the hydrogen rotation but also the flip motion of the water molecules, it is effectively coupled with the mode involving the translational motion.

In summary, we studied the hydrogen-bond rearrangement within a water dimer and its coupling to molecular vibration by using an STM. The molecules in a dimer exchange their roles as hydrogen-bond donor and acceptor, and the rate was directly determined by monitoring the interchange events in real time. The large isotope effect was found between $(H_2O)_2$ and $(D_2O)_2$, suggesting that quantum tunneling is involved in the process. The excitation of donor-substrate stretch mode was found to effectively assist the interchange tunneling, highlighting the sensitivity of the interchange dynamics to the displacement of oxygen atoms.

The authors thank the Supercomputer Center, Institute for Solid State Physics, University of Tokyo for the use of the facilities. H. O. acknowledges valuable discussion with Professor Koji Ando.

---

*hokuyama@kuchem.kyoto-u.ac.jp

[1] T. R. Dyke, K. M. Mack, and J. S. Muenter, J. Chem. Phys. **66**, 498 (1977).
[2] R. S. Fellers, C. Leforestier, L. B. Braly, M. G. Brown, and R. J. Saykally, Science **284**, 945 (1999).
[3] N. Pugliano, J. D. Cruzan, J. G. Loeser, and R. J. Saykally, J. Chem. Phys. **98**, 6600 (1993).
[4] V. A. Ranea, A. Michaelides, R. Ramírez, P. L. de Andres, J. A. Vergés, and D. A. King, Phys. Rev. Lett. **92**, 136104 (2004).
[5] T. Mitsui, M. K. Rose, E. Fomin, D. F. Ogletree, and M. Salmeron, Science **297**, 1850 (2002).
[6] Y. Morikawa, Phys. Rev. B **51**, 14 802 (1995).
[7] J. Tersoff and D. R. Hamann, Phys. Rev. Lett. **50**, 1998 (1983).
[8] A. Kokalj, Comput. Mater. Sci. **28**, 155 (2003). Code available from http://www.xcrysden.org/.
[9] In the calculation, the water dimer along the [001] direction (bridging the atomic rows) has comparable binding energy (58 kJ/mol). This configuration is, however, ruled out by the STM images, and thus we propose the former structure.
[10] S. Meng, E. G. Wang, and S. Gao, Phys. Rev. B **69**, 195404 (2004).
[11] A. Michaelides and K. Morgenstern, Nat. Mater. **6**, 597 (2007).
[12] R. L. Redington, J. Chem. Phys. **113**, 2319 (2000).